Biochimica et Biophysica Acta 1828 (2013) 1754–1764

Contents lists available at SciVerse ScienceDirect

Biochimica et Biophysica Acta

journal homepage: www.elsevier.com/locate/bbamem

Cholesterol favors the emergence of a long-range autocorrelated fluctuation pattern in voltage-induced ionic currents through lipid bilayers

Natalia A. Corvalán, Jackelyn M. Kembro, Pedro D. Clop, María A. Perillo *

Instituto de Investigaciones Biológicas y Tecnológicas (IIBYT), CONICET—Cátedra de Química Biológica, Departamento de Química, Facultad de Ciencias Exactas, Físicas y Naturales, Universidad Nacional de Córdoba, Córdoba, Argentina

ARTICLE INFO

Article history:
Received 26 October 2012
Received in revised form 12 March 2013
Accepted 22 March 2013
Available online 29 March 2013

Keywords:
Black lipid membranes
Lipid pores
Ionic current
Detrended fluctuation analysis
Cholesterol

ABSTRACT

The present paper was aimed at evaluating the effect of cholesterol (CHO) on the voltage-induced lipid pore formation in bilayer membranes through a global characterization of the temporal dynamics of the fluctuation pattern of ion currents. The bilayer model used was black lipid membranes (BLMs) of palmitoyloleoylphosphatidylethanolamine and palmitoyloleoylphosphatidylcholine (POPE:POPC) at a 7:3 molar ratio in the absence (BLM_0) or in the presence of 30 (BLM_{30}), 40 (BLM_{40}) or 50 (BLM_{50}) mol% of cholesterol with respect to total phospholipids. Electrical current intensities (I) were measured in voltage (ΔV) clamped conditions at ΔV ranging between 0 and ± 200 mV. The autocorrelation parameter α derived from detrended fluctuation analysis (DFA) on temporal fluctuation patterns of electrical currents allowed discriminating between non-correlated ($\alpha = 0.5$, white noise) and long-range correlated ($0.5 < \alpha < 1$) behaviors. The increase in $|\Delta V|$ as well as in cholesterol content increased the number of conductance states, the magnitude of conductance level, the capacitance of the bilayers and increased the tendency towards the development of long-range autocorrelated (fractal) processes ($0.5 < \alpha < 1$) in lipid channel generation. Experiments were performed above the phase transition temperature of the lipid mixtures, but compositions used predicted a superlattice-like organization. This leads to the conclusion that structural defects other than phase coexistence may promote lipid channel formation under voltage clamped conditions. Furthermore, cholesterol controls the voltage threshold that allows the percolation of channel behavior where isolated channels become an interconnected network.

1. Introduction

One of the prominent membrane functions is the regulation of the transport of ions or other molecules. Ions have substantial energetic barrier to be transferred from water into the membrane. However, the energy of ions in a membrane decreases due to the presence of restricted water domains between lipids [1] and pores (channels) of high dielectric permittivity [2]. In textbooks [3], channels are mostly conceived as intrinsic membrane proteins gated by specific ligands [4], voltage-gated [5] or mechanically activated [6]. The ability of the lipid environment to modulate the activity of proteinaceous channels has been acknowledged [7], however, the lipid part of the membrane is mainly considered a permeability barrier for polar compounds and mere electrical insulator [3]. Conversely, for more than 40 years it has been known that pure lipid membranes in their chain melting regime and phase coexistence can be highly permeable to water, small molecules and ions [8,9].

Voltage-induced currents across pure lipid membranes exhibit discrete ion conduction events similar to proteins [10,11]. Hence, the concept of lipid ion channels (pores) has been coined to described this behavior in pure lipid bilayers where they were induced experimentally [2,12–15] and simulated through molecular dynamics [16]. Based on the conductance value and its dependence of the ion size, the radius of the average lipid pore formed in phospholipidic membranes was estimated as 1 nm [17]. Conversely, lipid mixtures containing ceramide are able to form channels large enough to translocate proteins [18]. A working model describes ceramide channels as columns of ceramide monomers that span the membrane and assemble to form a barrel-like structure [19].

The similarity between the quantized conductance and ionic current fluctuation pattern exhibited by protein free membranes and that what is considered to be due to protein channels led to propose that "the theoretical description of channels would lie in the thermodynamics of the membrane and its cooperative phase behavior rather than in the geometry of individual protein" [2]. On the same line of reasoning, the remarkable cholesterol concentration dependency of the activity of the human erythrocyte glucose transporter [20] has been considered an example of a regulatory effect of membrane lateral order, but it might also be suspected as a case of membrane permeability increase due to membrane packing defects at a phase coexisting condition.

Abbreviations: BLM, black lipid membrane; bSM, synaptosomal membranes purified from bovine brain cortex; CHO, cholesterol; DFA, detrended fluctuation analysis; POPC, palmitoyloleoylphosphatidylcholine; POPE, palmitoyloleoylphosphatidylethanolamine

* Corresponding author. Tel.: +54 351 4344983x5.
E-mail address: mperillo@efn.uncor.edu (M.A. Perillo).

0005-2736/$ – see front matter © 2013 Elsevier B.V. All rights reserved.
http://dx.doi.org/10.1016/j.bbamem.2013.03.019

Lipid ion channels appear in an asymmetrically stressed membrane. Charge imbalance [16] or the application of low-voltage, long-duration electrical pulses induce rearrangements of the membrane components that ultimately lead to the formation of aqueous hydrophilic transient pores [17]. However, for some high values of transmembrane voltage, irreversible electrical breakdown occurs with the consequent irreversible membrane rupture, by one or more supercritical pores formation that expand to the membrane boundary [21].

Currently, the phenomenon of voltage-induced lipid ion channels is vigorously debated among researchers who are interested in the study of specific ion channel conductivity and those who are attracted mainly by the study of natural and artificial membranes. For both the black lipid membrane (BLM) represents a useful model and in some cases is the model of choice. Thus, BLM electrophysiology provides several distinct advantages for these studies, including control of the constituents on either side of the membrane, manipulation of lipid composition, and the ability to study rare or challenging channels inaccessible to patch-clamp methods. In addition, studies on the BLM model may contribute to the understanding of several biologically relevant processes, including fusion, lysis, and apoptosis of cells that, as well as electrical cell activity, also involve an opening of a lipid pore and interestingly, have been shown to involve non-lamellar structures [22].

There are evidences that the presence of non-bilayer forming phospholipids (i.e. PEs or cardiolipin) is also essential for the activity of peripheral and integral membrane proteins [23–25]. It has been proposed that these phospholipids might modulate the protein function since they exert different lateral pressure at different depth of the bilayer [25]. In particular, the binary mixture composed of phospholipid mixture 1-palmitoyl-2-oleoyl-sn-glycero-3-phosphoethanolamine (POPE) and 1-palmitoyl-2-oleoyl-sn-glycero-3-phosphocholine (POPC) has been widely used to build up BLMs for protein channel reconstitution [26–28] but, up to our knowledge, the ion permeability exhibited by this type of lipid matrix perturbed through the application of a transmembrane voltage potential, has not received deep attention. The polar group of PEs forms intermolecular hydrogen bonds which provide unique properties to the hydration network at the lipid water-interface [29,30] and may play an important role in defining the pore formation tendency and consequently the conducting properties of these bilayers.

Beyond the membrane model and composition, in studies on membrane pore formation tendency and conducting behavior, the type of data analysis may be crucial to display the emergence of the complexity underneath the phenomenon under investigation. It is well established that the shape and duration of biological membrane electrical events fluctuate in time [31]. Focus has been centered on fluctuations from individual proteinaceous ionic channels, in particular, the temporal sequence of open and close times. Traditionally, it is considered that proteinaceous ionic channels present few possible states and that the probability of switching from one state to another depends only on the present state of the channel (i.e. is random; not autocorrelated) [32]. Frequently, fluctuations on different time scales may appear to be self-similar, in other words, the magnitude and rate of events may fluctuate over many temporal scales [31], show time series with fractal characteristics and memory, and could be considered fractal noise [33]. A large body of experimental and computational evidence [31,32,34–39] indicate that at least some proteinaceous ionic channels and other proteins exhibit significant memory effects (long-range autocorrelations) and fractal dynamics (for reviews see [31,32]). Moreover, fluctuations in membrane conductance (in the absence of proteinaceous ionic channels) also can present non-random dynamics [40] mainly under certain conditions, for example by applying a voltage step of sufficiently high amplitude [17]. To our knowledge, the conditions that favor the appearance of long-range correlations and fractal dynamics in lipid membranes, associated with voltage changes and cholesterol concentration, have not been systematically studied.

Thus, in the present work we studied voltage-induced ion current fluctuations in a phospholipid binary mixture of POPE:POPC in a 7:3 molar ratio, in the absence or in the presence of cholesterol (CHO). To get closer to the molecular complexity of a biomembrane, the behavior of a complex mixture of lipids extracted by the Folch–Lees method [41] from bovine brain cortex was also analyzed. The main objective was to achieve a global characterization of the temporal dynamics of the ion current fluctuation pattern under the hypothesis that it encodes some aspects of the membrane structural dynamics.

2. Materials and methods

2.1. Materials

1-Palmitoyl-2-oleoyl-sn-glycero-3-phosphoethanolamine (POPE), 1-palmitoyl-2-oleoyl-sn-glycero-3-phosphocholine (POPC) and cholesterol (CHO) were obtained from Avanti Polar Lipid, Inc. (Alabaster, Alabama). HEPES was from AppliChem GmbH (Darmstadt, Germany), n-decane from Mallinckrodt (Paris, KY, USA), KCl was from Merck (Darmstadt, Germany) and solvents (chloroform and methanol, HPLC grade) were from Sintorgan S.A. (Argentina).

2.2. Lipid source and solution preparation

Lipids used were either synthetic or became the lower phase of a Folch's partition [41] of synaptosomal membranes purified from bovine brain cortex (bSM).

bSM were obtained as described previously [42]. Briefly, meninges were eliminated, the cortex dissected, and the bSM were purified essentially according to the method of Enna and Snyder, modified by Perillo and Arce [43], lyophilized and stored at −20 °C. Immediately before use, membranes were resuspended in 20 volumes of 2:1 (v/v) chloroform/methanol. Then, 0.2 volumes of water were added to achieve a 2-phase separation. The upper phase and the interface were eliminated. The solvent of the lower phase was evaporated and the residual lipids were resuspended in n-decane.

Stock solutions of synthetic lipids in 2:1 v/v chloroform/methanol stored at −20 °C were mixed immediately before used to obtain a 7:3 mol/mol POPE: POPC binary mixture with 0, 30, 40 or 50 mol% of cholesterol (CHOL) with respect to total phospholipids. Solvent was evaporated under a stream of nitrogen and n-decane was added to reach a ~20–25 mg/ml final total lipid concentration.

Controls made in Langmuir films evidenced that n-decane was expelled from a monolayer when it reached ~30 mM/m. This lateral surface pressure is close to what is considered the equilibrium lateral pressure of bilayers ([44], see Supporting information).

2.3. Planar lipid bilayers

Planar lipid bilayers (BLMs) composed of phospholipids with different cholesterol content (BLM_0, BLM_{30}, BLM_{40} and BLM_{50}) or bSM (BLM_{bSM}) were formed, with the aid of a thin glass rod, by painting with the lipid solution over a circular hole (150 μm diameter) sculpted in the polystyrene cuvette of a bilayer chamber (model BCH-13A, Warner Instruments Inc., Hamden, CT). The cuvette was inserted into a polyvinylchloride holder, thus defining a wall and two aqueous compartments separated by a planar lipid film as was described previously [5,45]. Prior to bilayer formation, the hole was "coated" with a small quantity of the lipid cocktail on the *cis* side of the wall and was allowed to dry before adding solutions to the chambers. Both compartments, *cis* and *trans*, were filled symmetrically with 10 mM HEPES, 150 mM KCl and pH 7.4 electrolyte solution. Electrical connections were made via 2% (w/v) agar salt bridges in 200 mM KCl into each chamber, and silver–silver chloride electrodes. High ionic strength salt bridges are used to minimize liquid junction potentials [46]. To avoid mechanical vibrations and interference from electric fields during the measurement, the bilayer chamber with two Ag/AgCl electrodes in the *cis* and *trans* compartment

was placed in a Faraday cage on a mechanically isolated support. All experiments were carried out at 23 °C.

2.4. Electrical recording

Electrical recordings were performed with a BC-525D Bilayer Clamp Amplifier (Warner Instruments, Inc., Hamden, CT), with a 10 GΩ feedback resistor. Gain settings varied from 1 to 10 mV/pA. Analog output current signals were low-pass filtered at 10 kHz (−3 dB) with a four-pole Bessel type filter and digitized by an analog-to-digital converter (Data Acquisition Interface, InstruTECH ITC-18, HEKA Instruments, Inc., Bellmore, NY). Currents were acquired using PATCHMASTER software (HEKA Instruments, Inc., Germany). Data were analyzed using the program provided by HEKA Instrument, Inc. (Bellmore, NY). Baseline adjustment was determined by subtracting the zero fixed value. Data were filtered with a 200 or 700 Hz low-pass Gaussian filter. Original data (not filtered) and data filtered with low-pass Gaussian and Butterworth filters were submitted to a detrended fluctuation analysis (DFA) (see below) and results were compared, but no difference in the self-similarity parameter (α) values was observed (data not shown).

2.5. Detrended fluctuation analysis (DFA)

The current intensity time series were submitted to a fractal analysis, as described in detail elsewhere [47,48]. This method, based on the Hurst exponent, has been introduced by [49] to analyze the organization of DNA sequences. Since then, it has been used to analyze temporal series data of many different origins. The advantage of DFA compared with other fluctuation analysis is its applicability to non-stationary time series.

Briefly, in DFA a self-similarity parameter (α-value) was calculated as the slope of a Log–Log plot of fluctuation (Log F(n)) vs. windows size (Log n) for n within the range 290 (Log n = 2.46) and 2600 (Log n = 3.455) data points. Where F(n) (Eq. (1)) is the root square of the mean quadratic deviations of each y_i value with respect to the regression line $\hat{y}_{i,k}$ within the corresponding window (k).

$$F(n) = \sqrt{\frac{\sum_{i=1}^{N}\left[y_i - \hat{y}_{i,k}\right]^2}{N}}. \quad (1)$$

α-Value provides a measure of the "roughness" of the original time series: the larger the value of α, the smoother the time series [50]. Also, in DFA the exponent α is inversely related to a typical fractal dimension, so in this case, the value increases with increasing regularity (or decreasing complexity) in the time series [51]. Different values of the exponent α signify different levels of temporal correlation in fluctuation at different scales. For time series of processes where fluctuations are negatively correlated ("anti-persistent" noise) we have $0 < \alpha < 0.5$. For time series with consecutive values generated by statistically independent processes with finite variances, $\alpha = 0.5$ (uncorrelated or "white" noise); in this case data has short-range correlations (i.e., the correlations decay exponentially). $0.5 < \alpha < 1$ corresponds to processes where fluctuations in subsequent values are positively (long-range) correlated ("persistent" noise) and correlations decay as a power-law meaning that ongoing behavior is influenced by what has occurred in the past [52]. $\alpha = 1$ corresponds to power spectral 1/f noise which is typical of systems near self-organized critical states [53]. Values of α in the range $1 < \alpha < 1.5$, correspond to integrated negatively correlated ("anti-persistent") noise, where $\alpha = 1.5$ ("brown" noise) correspond to integrated independent increments of "white" noise [31].

2.6. Frequency distribution of opening times

Timescales were characterized on the same set of data used to describe the effect of ΔV and CHO content H = on conductance. The threshold criterion applied was that the cut-off frequency of the low pass filter was set individually for each experiment to be at least ten times higher than the sampling frequency. Frequency distribution of opening times was analyzed by plotting the frequency vs. the duration of open events, respectively in a double logarithm scale. We evaluated whether the frequency distributions adjusted to linear fits in Log–Log plots. When a linear fit coefficient of determination (r^2) was found to be higher than 0.7, it was considered that the distribution was likely representative of a power-law (and therefore fractal) distribution [54]. The slope of the linear fit is known as the scaling factor (β).

2.7. Statistical analysis

Regression analysis by the least squares method used for curve fitting and Kruskal–Wallis H test applied for comparisons were performed by using the InfoStat software [55].

3. Results

Representative transmembrane ionic current recordings and their respective amplitude histograms obtained with BLM_0 upon application of holding potentials (ΔV) within the range ±200 mV, are shown in Fig. 1. States of discrete conductance were observed at $\Delta V \leq -140$ mV, while a short-lived spike-like behavior was frequent at $\Delta V \geq 140$ mV.

Most of the observed changes in conductance were abrupt transitions from one conductance level to another. The transition to a new level of conductance was often followed by a return back to the initial conductance within a few milliseconds. The abruptness of the transitions and the closeness of the initial and final levels of conductance suggest that these fluctuations reflect opening and closure of single lipid pores. Moreover, we observed another type of electrical activity, conductance steps, at the highest potentials tested (e.g. trace at −200 mV in Fig. 1) mainly in samples containing 40 and 50 mol% CHO. In this case, after abrupt establishing of a new conductance level, this level was stable for up to several hundred milliseconds. (Typical traces of electrical current vs. time recorded in BLMs containing CHO are depicted in Fig. 1Sa in the Supplementary data).

Histograms of counts number (N) vs. current intensity (I) show the presence of one or more characteristic current amplitude values (I) that increase in magnitude and number as a function of the holding potential (ΔV) (Fig. 1, right panels). In addition, the application of positive and negative potentials led to differences in the pattern of current fluctuation (Fig. 1) as well as in the number of conductance states (more numerous for negative potentials) (Fig. 2) suggesting different behavior for K^+ and Cl^- ions.

The current amplitude (I) vs. the holding potential (ΔV) plots for BLM_0, BLM_{30}, BLM_{40} and BLM_{50} are shown in Fig. 2a–d and the corresponding conductance values are depicted in the insets of Fig. 2a–d. In BLM_0 (Fig. 2a) the current amplitude and the number of conductance states increased at $|\Delta V| > 120$ mV up to values above ±200 pA. Within the range 0 to ±100 mV, a single conductance state (G = 0.0694 ± 0.0210 nS) was observed (Fig. 2a inset). A similar behavior was observed for BLM_{30} (Fig. 2b) where current amplitudes for $|\Delta V| > 100$ mV increased up to −350 pA at −160 mV and 200 pA at 200 mV (Fig. 2b). The highest absolute I value at each ΔV ($I_{max,V}$) increased almost linearly with ±ΔV for bilayers of BLM_{40} (Fig. 2c) with $I_{max} \approx \pm 800$ pA at 160 and −140 mV, leading to a maximal conductance of 5 and 6 nS, respectively. In the case of BLM_{50} (Fig. 2d) I values were very dispersed, the highest I values reached were within a similar level as those reached by BLM_{40} but without a clear pattern.

Capacitance (C_m) values increased symmetrically with respect to ±ΔV although a slight asymmetry was observed in BLM_0 with values

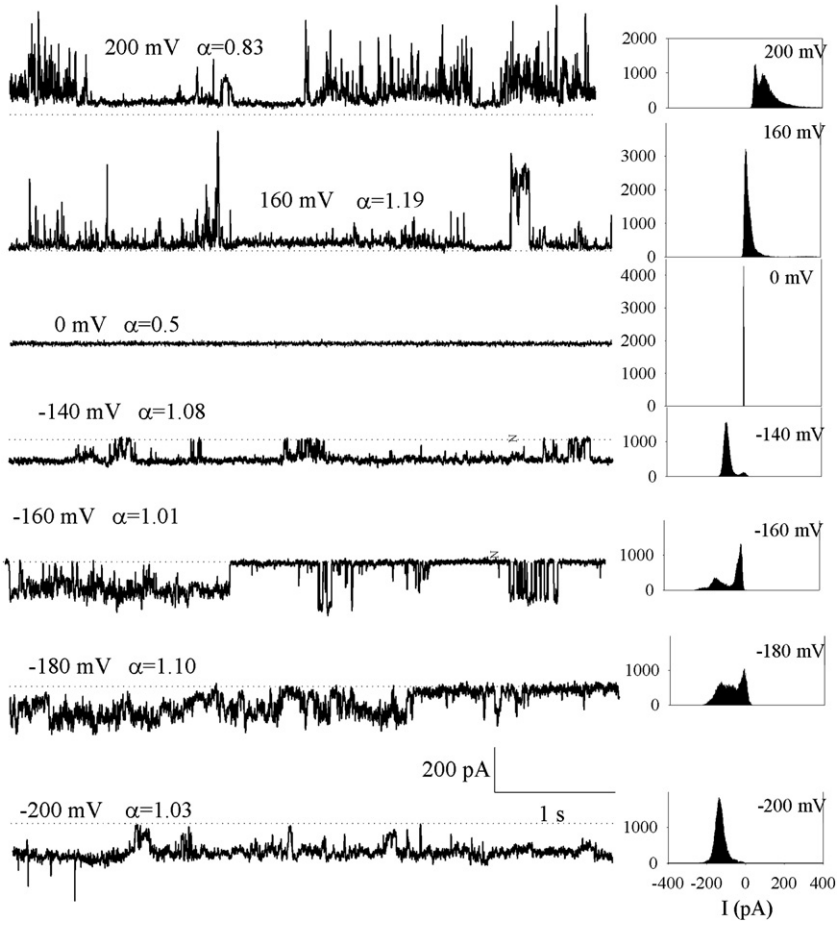

Fig. 1. Voltage-induced temporal fluctuation pattern of ionic currents across POPE:POPC (7:3) planar bilayer membranes (BLM_0). Right panels, representative transmembrane ionic current recordings from planar bilayers composed of POPE:POPC (7:3) (BLM_{30}), upon application of a holding potentials between ±200 mV in the presence of symmetrical K^+/Cl^- (150 mM KCl). Dotted lines represent baselines, corresponding to 0 A current intensity. Recordings from 0 to ±120 mV show a similar behavior (data not shown). Left panels, all-points of amplitude histograms obtained by fitting a Gaussian distribution to experimental values.

tending to be higher at negative potentials compared with those calculated at positive potentials. C_m also increased systematically as a function of x_{CHO} (Fig. 3a). Variation of C_m with ΔV ($C_{m(V)}$) followed the equation $C_{m(V)} = C_{(0)}(1 + \alpha \cdot \Delta V^2)$, where $C_{(0)}$ is the capacitance at $\Delta V = 0$ and α the fractional increase in capacitance per square volt (note the underline used to differentiate form the self similarity parameter α). The quadratic ΔV dependence of C_m depicted in Fig. 3b indicates a constant α in the case of BLM_0 which is consistent with Alvarez and Latorre [56,57]. However, the behavior in the presence of CHO was clearly biphasic exhibiting an abrupt slope (α) change at $\Delta V \cong \pm 180$ mV (Fig. 3b). Below ±80 mV, α increased significantly as a function of CHO while above ±80 mV only slight changes in α were observed (Fig. 3c).

The strong variability observed among current recordings obtained in similar conditions led us to investigate the complexity underneath this phenomenon through DFA. In Fig. 4a raw data of three temporal recordings of I and a fourth one coming from the randomization of one of the formers are shown. Determination of the self-similarity parameter α from the slope of the F(n) vs. n in Log–Log plot are depicted in Fig. 4b. This procedure was systematically applied to DFA on the temporal fluctuation pattern of ion currents across BLMs composed of POPE:POPC (7:3) with or without CHO (Fig. 5a–d). Due to the characteristic variability, in each experimental condition we analyzed fluctuation patterns obtained from the many replicates (up to 10 in some cases). BLM_0 (Fig. 5a) showed α values at or slightly above 0.5 within ±100 mV, indicating short range correlations or white noise. Fluctuations in this range are clearly due to stochastic events occurring at the membrane level, determined, for example, by the fluctuation in thermodynamic variables of the lipid bilayers. Beyond −140 and +160 mV most of the BLM_0 analyzed suffered a transition to 1/f-type noise (α tended to one). In $1/f^b$ noise ($b = 1$), there is no well-defined temporal scale for the correlation time and the autocorrelation function decays as a power law. That is, the current value of the measured signal is temporally correlated not only with its most recent value but also with its long-term history (i.e. long-range autocorrelations) in a scale-invariant, fractal manner [58]. In the other BLMs, the range with $\alpha \sim 0.5$ became narrower as the proportion of cholesterol increased. Thus, BLM_{30} (Fig. 5b) showed long-range correlations ($0.5 > \alpha = 1$) when ΔV was beyond −50 mV and +130 mV. The α vs. ΔV plot in BLM_{40} and BLM_{50} membranes resembled an upward parabola centered at 0 mV. In BLM_{40} (Fig. 5c) and BLM_{50} (Fig. 5d) long-range autocorrelations were observed even at $\Delta V = 0$ mV, but the probability of finding $0.5 > \alpha \cong 1$ increased with the magnitude of the electrical potential.

Pore lifetimes were also analyzed statistically. Fig. 6a is a histogram on a Log–Log scale showing the frequency of occurrence of the different pore lifetimes in a BLM_{30} clamped at −160 mV taken as an example. The plot exhibits a straight zone along at least two decades with a slope (β) being a self-similarity parameter which measures the degree of autocorrelation of pore lifetimes. The large range of these times, which cannot be represented by one scale, is characteristic of a fractal [32].

Finally, we analyzed the temporal fluctuation of ionic currents across BLMs composed of a complex mixture of lipids from the Folch's lower phase of brain synaptosomal membranes (BLM_{bSM}). Fig. 7a shows that in BLM_{bSM} I_{max} rose with ΔV only up to ±20 pA at ±200 mV and reached an average conductance $G \approx 60$ pS. These values were similar to those measured in BLM_0 within the ΔV range ± 100 mV ($G \sim 40$ pS) but significantly lower than the highest values reached in BLM_0 at higher

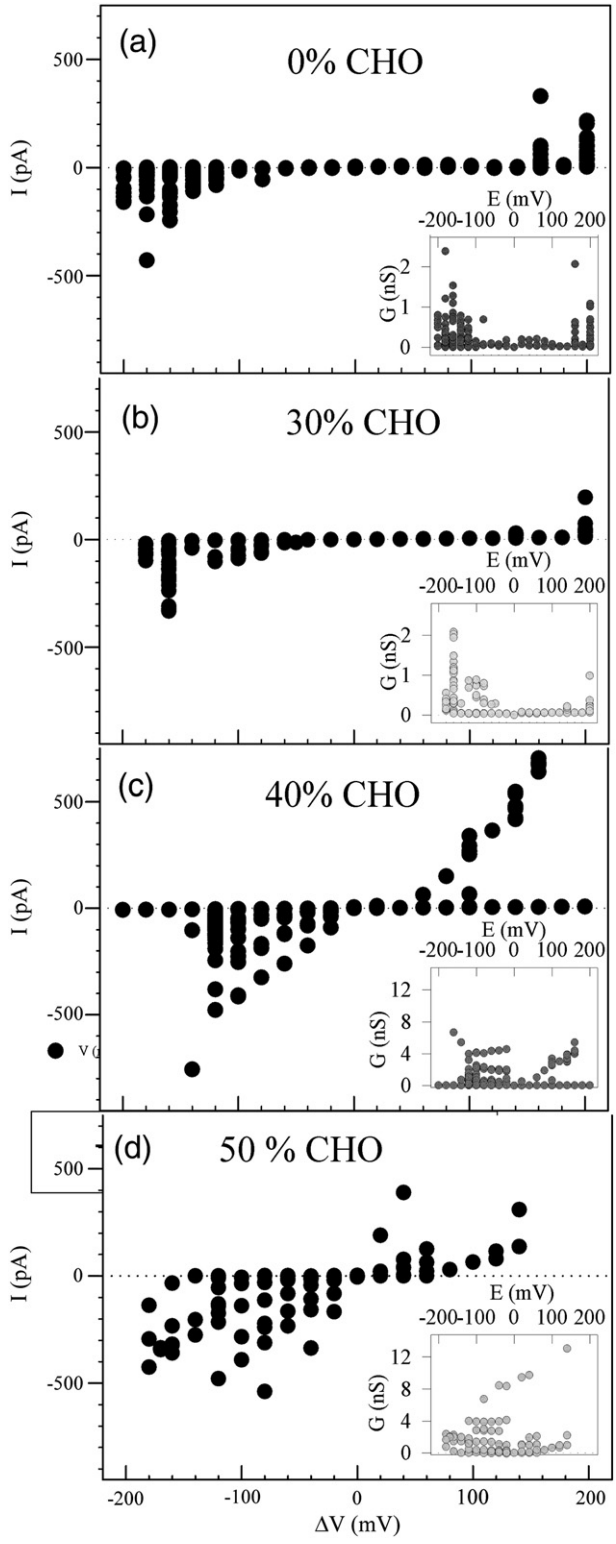

Fig. 2. Effect of cholesterol on current intensities and conductance states. Current-electrical potential plots (I–ΔV) (a–d) and conductance vs electrical current plots (G–ΔV) (a–d insets) across POPE:POPC (7:3) BLMs containing from 0 to 50 mol% cholesterol with respect to total phospholipids. Conductance states were identified from current amplitude histograms. Kruskal–Wallis analysis showed highly statistically significant effects of both voltage ($H_{[412,22]} = 94.53$, $p < 0.0001$) as well as CHO content ($H_{[388,4]} = 15.05$, $p < 0.018$) on current intensity.

potentials (1 nS). Current fluctuations in BLM_{bSM} followed a white noise behavior but tended to an autocorrelated behavior reaching $\alpha \cong 0.70$ at ΔV beyond −180 and +140 mV (Fig. 7b).

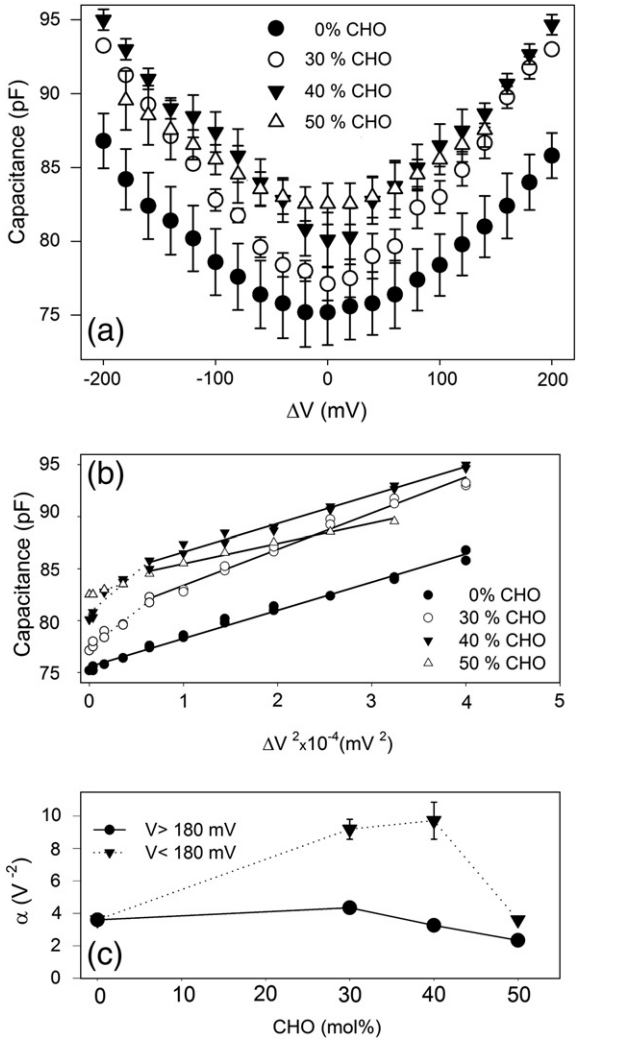

Fig. 3. Change in membrane capacitance (C_m). a) Effect of ΔV in BLMs containing increasing cholesterol (CHO) proportions. b) Change in C_m vs. increasing squared voltage potential (ΔV^2) from 0 to 200 mV at the indicated CHO content in the BLM formulation (calculated from data in panel). c) α was estimated from the slopes of plots shown in panel b within the 0–80^2 mV^2 and 80^2–200^2 mV^2 ranges, respectively. For data a Kruskal–Wallis analysis showed highly statistically significant effects of both voltage ($H_{[310,21]} = 124.71$, $p < 0.0001$) as well as CHO content ($H_{[310,4]} = 56.51$, $p > 0.0001$) on capacitance values.

4. Discussion

Thus, in the present work we studied the phenomenon of voltage-induced lipid ion channels in a membrane model containing a lipid with negative spontaneous curvature. This kind of lipids can be organized in non-lamellar structures participating in the opening of lipid pores which are relevant for many biological functions beyond the transmembrane ion permeability. Even though the lipid mixture studied here is extensively used for protein channel reconstitution, up to our knowledge its behavior in the BLM model has not been analyzed thoroughly neither alone nor in the presence of CHO. Another aspect approached here, is the ion conducting behavior of a complex mixture of lipids extracted from a natural membrane. This may be relevant to evaluate the limits of simplified membrane models at reproducing the behavior of a natural biomembrane. Temporal fluctuations of ion currents were submitted to a global analysis aiming at uncovering a characteristic pattern and its correlations with the membrane structural dynamics.

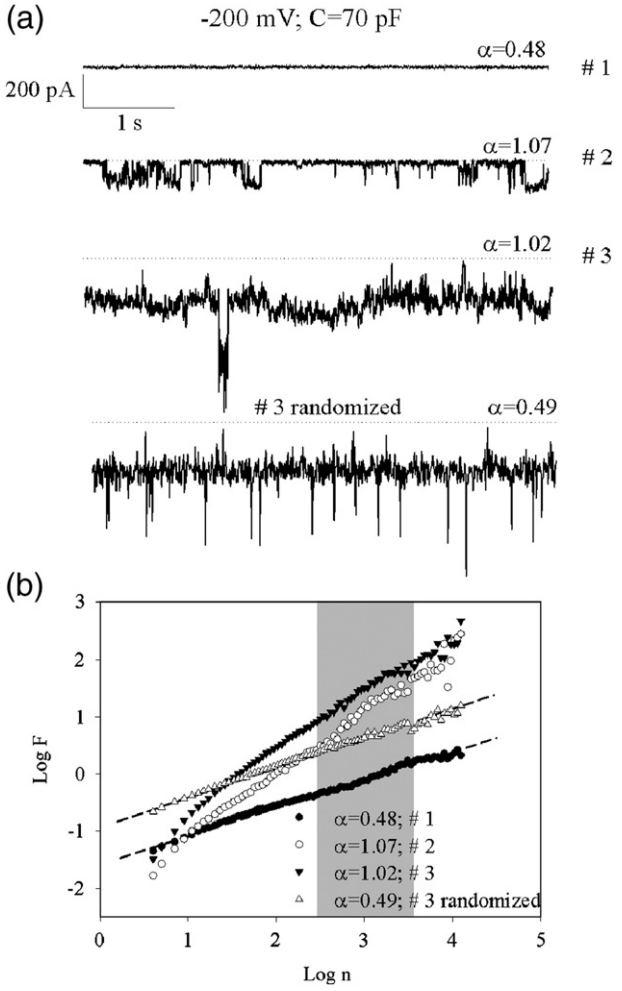

Fig. 4. Determination of self-similarity parameter α from detrended fluctuation analysis (DFA). (a) Current traces at 200 mV in POPE:POPC (7:3) BLMs. Trace #4 resulted from the randomization of trace #3. (b) DFA on current patterns shown in panel (a). Note the remarkable variability in the shape of current fluctuation patterns obtained under similar experimental conditions. The self-similitary parameter (α-value) is calculated for window sizes in the range 290 (Log n = 2.46) and 2600 (Log n = 3.455) data points (gray region).

4.1. Change in the membrane capacitance

Beyond electrostatic properties of the membrane surface and interior, capacitance may provide information about membrane structure and geometry. Typical capacitances of membranes have been claimed to be between 0.6 and 1 μF/cm^2 [2]. In the present work a minimum of 66 pF (in BLM_{bSM} at 0 mV) and maximum 95 pF (in BLM_{50} at 200 mV) were found (Fig. 3), equivalent to 0.37 and 0.54 μF/cm^2 specific capacitances, respectively. These values, as well as the increasing tendency in C_m upon membrane rigidization, are in accordance to those reported by Antonov et al. [59] who found an average specific capacitance of the hydrogenated egg-lecithin BLM of 0.73 μF/cm^2, which was nearly twice as much as that for BLM formed from native egg lecithin.

We found that CHO induced an increase in C_m even at 0 mV (Fig. 3a), a deviation from the straight line in the quadratic ΔV dependence of C_m, a CHO dependent increase in α within the 0–±180 mV voltage range and a recovery of the α values found for BLM_0 at $\Delta V \geq \pm 80$ mV. These results may be reflecting geometrical changes in BLM such as area and/or thickness changes associated to the electrostriction phenomenon (electrically caused decrease in thickness) and can be treated as White and Chang [57] by discriminating between the effects of ΔV on the intrinsic capacitance (β) and on the BLM area (B) through $\alpha = \beta + B$ [57]. This possible CHO-dependent molecular reorganization in the BLM seems to be completed at ~80 mV where BLM would reach electrostatic properties similar to those of a CHO free membrane. It has been calculated that C_m of a fluid phase is ~1.5 times larger than that of a gel phase while the voltage dependence C_m of a single phase is small [60], mainly in solvent-free membranes [56]. This is so because the in the gel–fluid phase transition there is an increase in area with respect to the gel phase which is higher than the decrease in membrane thickness. A similar

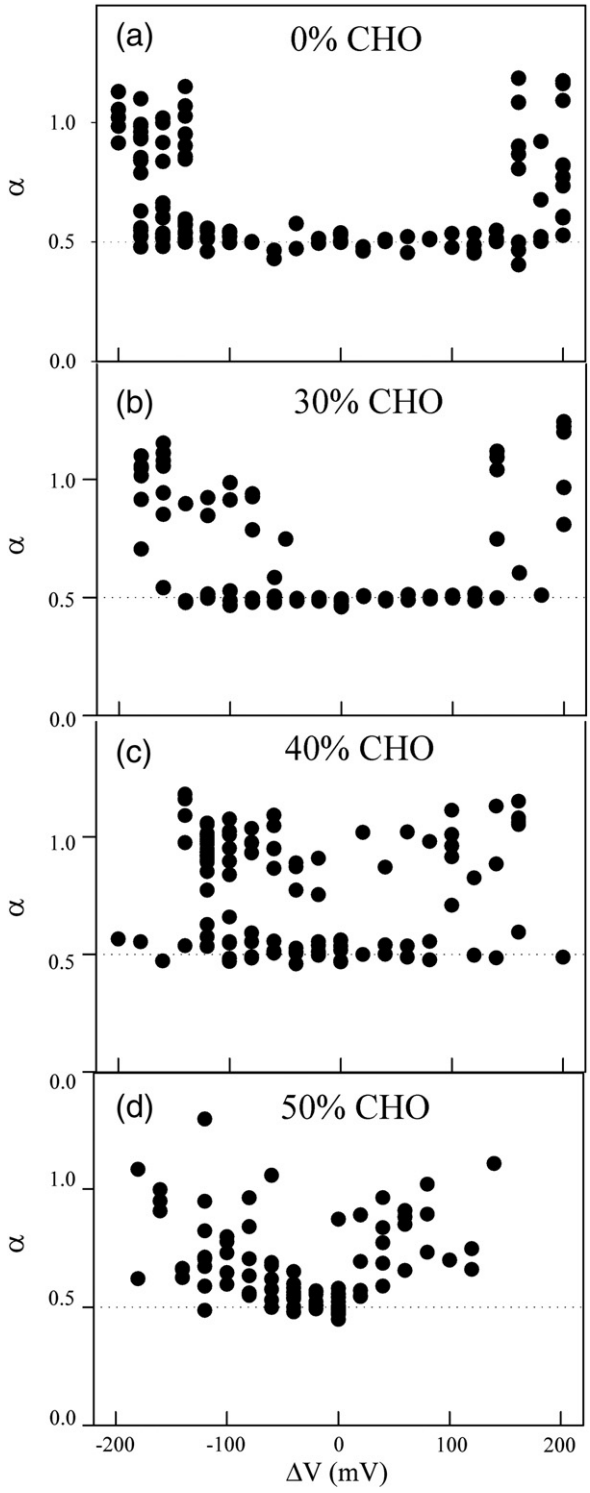

Fig. 5. Effect of cholesterol on the complexity of fluctuation patterns. Self-similarity coefficient (α) at different transmembrane potentials, estimated with DFA from electrical current fluctuations across POPE:POPC (7:3) BLMs containing from 0 to 50 mol% (a–d) cholesterol with respect to total phospholipids.

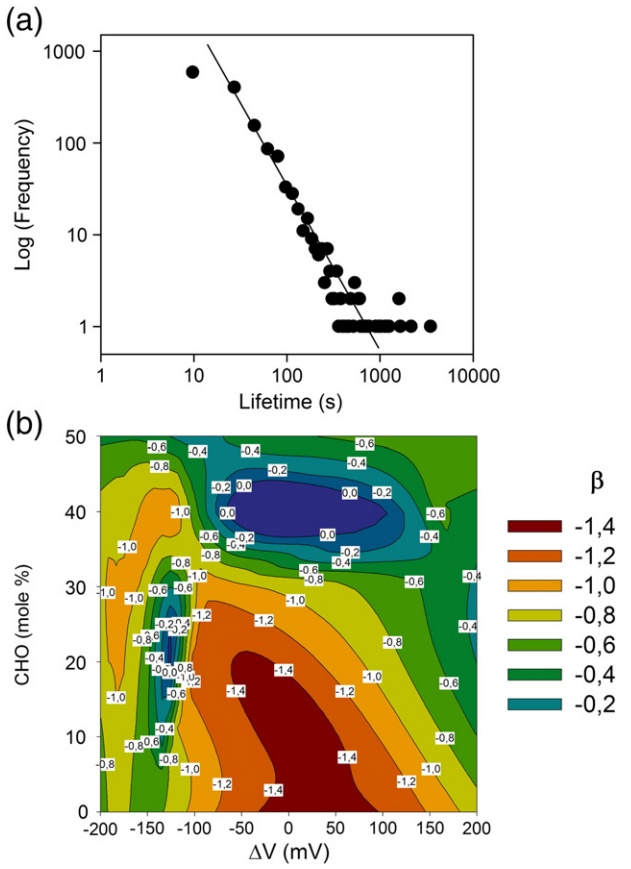

Fig. 6. Statistics of the open times. (a) A histogram on a Log–Log scale showing the rate of occurrence of the different pore lifetimes in a POPE:POPC (7:3) BLM containing 30 mol% cholesterol and clamped at −160 mV. The Log–Log plot reveals the power low distribution with a slope β, the autocorrelation parameter, that extends over at least two decades. (b) Contour plot showing the variation of β (represented by the color code) in different conditions of CHO content (mol% with respect to phospholipids) and transmembrane electrical potential (ΔV).

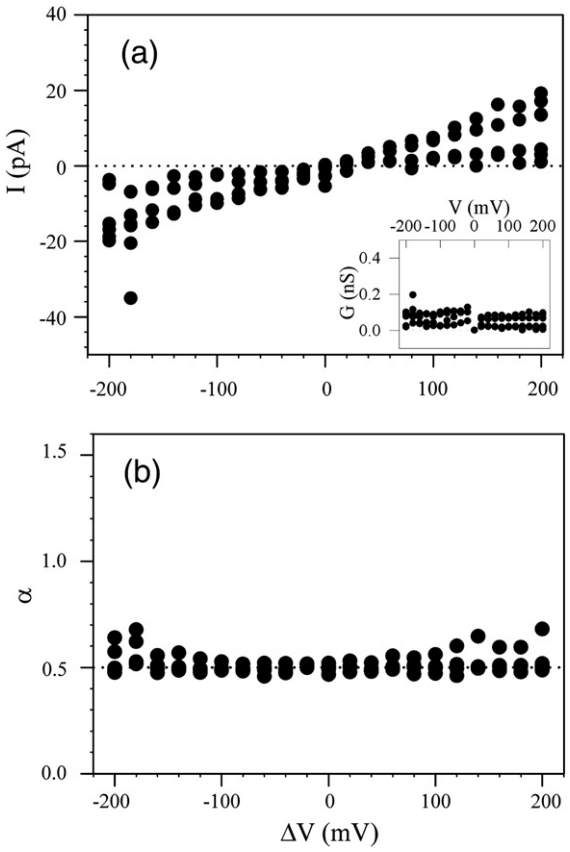

Fig. 7. Ionic currents through BLMs of bovine synaptosomal membrane lipids. BLMs were prepared with Folch's lower phase lipids. (a) Ionic current intensity and (b) self-similarity parameter α derived from DFA on current traces recorded over time at different transmembrane potentials. Kruskal–Wallis analysis on BLM_{bSM} showed statistically significant effects of voltage on I ($H_{[99,21]} = 85.87$, $p < 0.0001$) (panel a) but not on α values ($H_{[39,21]} = 15.80$, $p = 0.7290$) (panel b). In addition, BLM_{bSM} resulted significantly different from BLM_0 both in the I response ($H_{[320,2]} = 17.28$, $p > 0.0001$) as well as in the α values obtained ($H_{[207,2]} = 36.21$, $p < 0.0001$) as a function of the intensity of voltage applied.

rationale can be applied to analyze our system but only in qualitative manner because it cannot be referred to a gel phase in CHO containing mixtures. So, upon rising ΔV beyond ±180 mV, the higher C_m values (Fig. 3a) and mainly the decrease in voltage dependence of C_m (lower α) (Fig. 3c) suggest that due to electrostriction BLMs containing CHO suffered a decrease in both structural complexity and anisotropy. This rationale provides a plausible explanation to the voltage induced effects but not to the CHO dependent increase in C_m and α below ±80 mV. So, additionally to pure capacitive effects [60], a resistive effect should also be taken into account. From the expression: $C_m = \varepsilon_0 \cdot \varepsilon \cdot A/d$, where ε_0 is the permittivity in vacuum, ε the permittivity, d the monolayer hydrocarbon thickness and A the area, it can be concluded that the effect of increasing ΔV as well as that of increasing x_{CHO} on C_m would reflect not only a decrease in bilayer thickness but also an increase in the polarity of the membrane core (ε).

Phenomena affecting membrane thickness include not only electrostriction but also the local accumulation of material and local thickening of the membrane which is a likely immediate outcome of pore formation. However, both have negligible effects at low potentials. Furthermore, increase in membrane order at the hydrocarbon chain region can also cause an increase in membrane thickness. So, the effects of CHO on C_m observed in the present work could be interpreted based on the ability of this steroid to increase membrane order in liquid crystalline bilayers leading to a more rigid, thus extended, organization of hydrocarbon chains. We confirmed this behavior in POPE:POPC mixtures in Langmuir film experiments (see Fig. 5S, Supplementary data). It is worth noting that, the thickening of the bilayer structure during the phase transition of the BLM from the liquid crystal state to the gel state has been ascribed partly to a gauche-trans transition of lipid molecules but mainly due to redistribution of the solvent n-decane [59]. Contrary to this, our experiments on the mixing behavior of POPE:POPC with n-decane in Langmuir films, indicated that the solvent appears to be totally excluded from the monolayer at all lateral surface pressures (π). Even at π levels that are compatible with the equilibrium lateral pressure of bilayers there is no residual n-decane at the interface (see Fig. 3S, Supplementary data) possibly due to the fact that the isothermal experimental conditions above the melting point of n-decane contributed to its instability at the interface. So, it can be concluded that in our system the only source of significant effects on membrane thickness is CHO-induced membrane rigidity. However, it is expected to exert the effect opposite to that observed experimentally in Fig. 3a.

The effect of membrane polarity on C_m is reflected by changes in ε. Taking into account that the dielectric constant of lipid is $\varepsilon_L \cong 2$, that of the bulk water is ε_w(bulk) ≅ 80 while bound water has a smaller dielectric constant (e.g., ε_w(bound) ≅ 6–10) then, ε-dependent changes on C_m can be interpreted as follows. Water has been postulated to penetrate deeply into the membrane interior and to be organized into domains [61]. So, the amount and/or size of water domains are expected to define an average ε value of the membrane. This average ε, would define a threshold energy level for pore formation and would increase upon membrane perturbation (e.g. upon applying an electrical potential). So, the effect of ΔV on C_m can be partly explained on the basis of ΔV-induced growth in the size and number of water domains. CHO exerts a dual effect, on the one hand by decreasing C_m through the increase in membrane

thickness and on the other hand by increasing C_m though the induction of packing defects which stimulate water domains formation. Thus, the latter effect is underneath and overpassed in magnitude by the former and the net consequence is a CHO-induced increase in ε and consequently in C_m.

4.2. CHO content and high potentials favor auto-correlations in temporal fluctuation patterns of ion currents

After a systematic analysis of ion current fluctuations in different experimental conditions, the intrinsic variability as well as its varying tendencies with CHO content and voltage sign and intensity could be confirmed and interpreted as a fingerprint of the system (examples of I vs. time traces exemplifying the variability in current temporal fluctuation patterns are depicted in Fig. 1Sb, in the Supplementary data). Upon initial inspection, a time sequence of normal fluctuations in magnitude and rate of a measurable quantity appears irregular and completely random. By random it is meant that fluctuation are independent from one another, i.e., there is no apparent dependence or correlation among fluctuations. If, however, a sequence of events is considered, the fluctuations may look remarkably like those observed in shorter or longer sequences. That is, fluctuations on different time scales may appear to be self-similar, like the branches of a geometric fractal object [27]. In other words, magnitude and rate of events may fluctuate over many scales (Fig. 1Sc, Supplementary data), even in the absence of external stimuli that fluctuate, rather than relaxing to a homeostatic steady state.

So, aimed at uncovering long-range correlations associated to a scale invariant (fractal) behavior, ion current time series were submitted to a global analysis. Some of the experiments with BLM containing CHO exhibited a slow drift of the mean conductance and in some cases were accompanied by abrupt transitions between different conductance levels. This non-stationarity of conductance, which would have complicated other type of fluctuation analysis such as power spectrum, could be properly treated with DFA.

In the time series with long-range autocorrelations, many of the discrete steps in membrane current look similar to protein induced ion channels (Fig. 4). Previous studies have shown that ion currents through proteinaceous ionic channels can present long-range correlations with α-values > 0.5 and/or near 1. For example, patch clamp recording of the potassium current through a single high conductance locust potassium channel showed an $\alpha = 0.89 \pm 0.07$, indicating that the ionic current signal has long memory property (long-range correlations) [37]. Using other mathematical analysis, studies regarding proteinaceous ionic channels have also shown existence of $1/f^b$ noise ($b = 1$) [31,32,34,38,39]. Bier and Gallaher [40] discussed extensively 1/f noise both in protein channels and lipid pores. A model proposed by these authors considers that, once overpassed an opening energy barrier, the probability that the system closes again becomes lower as it moves away from the barrier. In lipid bilayers in the liquid state a pore would open (O) and close (C) rapidly. However, near the phase transition lipids in the pore lining may freeze stabilizing the pore. The freezing of more lipids around the pore moves the system away from the C⇆O energy barrier. According to this model, they propose a mechanism based on a closed–open transition (C⇆O) scheme where the transition rates (k) decrease in time like $k(t) = t^{-\beta}$ [40]. This considers the electropore noise within the general category of nonequilibrium systems in which energy is dissipated exhibiting a 1/f noise.

Interestingly, the voltage range and CHO concentration where long-range autocorrelated fluctuation pattern in voltage-induced ionic currents through lipid bilayers emerge (Fig. 5), closely resembles both the voltage range where an increased ion current through the membrane was observed (Fig. 2) and also the voltage range where abrupt transitions from one conductance level to another was found (Figs. 1 and 4). As stated previously, the abruptness of the transitions and the closeness of the initial and final levels of conductance suggest that these fluctuations reflect opening and closure of single lipid pores [17]. Therefore, our results suggest that fluctuations, due to the formation of lipid ion pores at extreme voltages and CHO concentrations, present fractal dynamics and long-range correlations (see Section 4.4 for detailed discussion). Based on their work as proteinaceous ionic channels Chui and Fyles [36] proposed, three possible mechanisms for which power law distributions (long-range autocorrelations, fractals) can arise. First, they could arise from a "combination of exponentials" process in which a conducting state would both grow and die off exponentially. The latter process is not unexpected and underlies the conventional Markov analysis where open-state lifetimes decrease exponentially [36]. A second and more appealing alternative is related to the properties of a "random walker". In this model the "walker" would be defined as a conducting state of a channel. This minimum conducting state would randomly add or subtract components. The conducting state would persist until the random add/subtract process produces a structure below the minimum required for conduction [36]. A third alternative involves "self organized criticality" in which the system as a whole grows in conductance by a random process. To counter this growth, a random catastrophic event hits this organized structure and wipes it out in its entirety [36]. For example, 1/f-noise was observed in open bacterial porin channels, and was attributed to a non-equilibrium critical state of the channel, where ion diffusion across the pore happens in differently sized "avalanches" of self-organized criticality [39]. Hausdorff and Peng [58] proposed that the 1/f fluctuations observed in many biological time series could result from the summation of multiple random inputs, although it is unlikely that these fluctuations are due only to the fact that these systems are regulated by many different inputs acting on different time scales [58]. Bier and Gallaher [40] arrive to a similar conclusion. Further studies are necessary to fully comprehend the mechanisms that underlie the appearance of 1/f-noise in voltage-induced ionic currents through lipid bilayers.

Heterogeneous lipid bilayers made of soybean lecithin, egg phosphatidylcholine and cholesterol also presented histogram of open times that showed conductance events ranging over several orders of magnitude, from 1 ms to as long as many seconds (the majority remained open for less than 10 ms) [62], although no information on the distribution of events was provided in the paper. More recently, Melikov, et al. [17] reported the presence of lipid pores with a broad distributions of lifetimes (up to 100 ms). They also showed that the histogram of the number of closed states in bursts confirms that the number of longer bursts containing many consecutive short-lived closed states is increased in comparison with that generated by computer simulation for independent events [17]. In our study, the self-similarity parameter (β) varied with transmembrane voltage as well as with BLM composition as shown in the contour plot of Fig. 6b. Noteworthy, less negative slope values (between −0.2 and −0.6) were found for higher voltages and higher CHO concentration indicating more events with longer pore lifetimes under these conditions.

4.3. Selectivity in ion permeability

Several pieces of information derived from the present study revealed an asymmetry in ionic conductance mainly reflected by the variability of data as well as the sensitivity of the system to perturbation which are the strongest within the negative voltage side of I–ΔV (Fig. 2) and α–ΔV (Fig. 5) plots.

Selectivity between anions and cations is known since the early work from Papahadjopoulos and Watkins [63] who showed that the $^{36}Cl^-/^{42}K^+$ diffusion ratio through PC vesicle bilayers was between 37 and 42. This value decreased near 10 times in the presence of CHO and even more in membranes containing negatively charged lipids such as phosphatidic or stearic acids. Taking into account that cations perturb the hydration layer of bilayers [64] and the ion size selectivity described by the conductance of different cations which is in accordance with the well-known Hofmeister series, it has been proposed that hydration force is the responsible for cation selectivity at soft-perforation [10].

More recently, Liontiadou et al. [65] reported plausible explanation for ion selectivity resulting from molecular dynamics simulations. They proposed that the sodium and chloride ions permeate the water pores via different mechanisms. Whereas sodium is adsorbed to the membrane and diffuses across the interface, chloride prefers the bulk water in the middle of the pore. Although the interface attracts the sodium ions, it also restricts their motion. As a consequence, the average time required for a chloride ion to pass through the pore results much shorter than for a sodium ion and upon increasing the pore size, a reversal from cation to anion selectivity is observed.

4.4. Electrical potential and membrane structure dependence of lipid pores percolation tendency

Fluctuation analysis based on current intensity as well as on pore lifetimes can be rationalized as pores behaving independently at low voltages in BLM_0, at the edge of the fluid state (above the mean phase transition temperature) as it is in the present study. As voltage (and CHO concentration) increases, pores start to feel each other, either because they become bigger or because their conducting effects diffuse across space and ionic currents from neighboring pores become in contact. This spatially self-organized behavior grows up to the point where it expands (percolates) to the whole membrane and is expressed as temporally correlated fluctuation in ionic currents. At extreme conditions membrane breaks up. Our results (Fig. 5) show that percolation (α tending to 1) can be achieved at lower voltages, thus requiring less energy, in membranes containing CHO.

Ion channels are described as hydrophilic defects produced as a consequence of the thermodynamic fluctuations in the two-dimensional phospholipid lattice which are considered to be maximum at the melting transition [2]. However, in the fluid phase Wunderlich et al. [15] have described spike-like fluctuation within timescales (~2 ms), one order of magnitude shorter and of narrower amplitude than those observed in phase coexistence conditions. Interestingly, although all the mixtures assayed in the present work were above their phase transition temperatures they showed fluctuation within timescales above 10 ms. This suggests that, in spite they are not expected to exhibit phase coexistence, other type of packing defects should be considered.

PC and PE differ considerably in their effective sizes, hydration properties, and inter-hydrogen bonding capability of their polar headgroups as well as their intrinsic curvatures pertinent to the effective structure and intermolecular interactions of lipid molecules in membranes. It is known that the physical properties of fluid PE/PC do not vary smoothly with PE composition. Abrupt, albeit not major, deviations appear to occur at particular critical PE compositions [66]. POPE:POPC mixtures have been shown to form headgroup superlattice in fluid bilayers at certain critical proportions (e.g. 0.667 which is very close to that used in the present paper). Headgroup superlattice model assumes that the lipid headgroups form hexagonal or rectangular superlattice distributions in the bilayer, a mechanism that relieves "packing frustration" of PE in the presence of PC (larger headgroup than PE) [66]. Hence, this may be one of the major mechanisms in driving the PE and PC components to superlattice-like lateral distributions in the bilayer [66].

The formation of the putative CHO superlattices in fluid PC host bilayers [67] has also been described as a mechanism responsible for repulsive steric interactions at the hydrocarbon level. In turn, CHO supports formation of phospholipid headgroup superlattices in fluid state ternary lipid bilayers (e.g. when the CHO-to-phospholipid mole fraction (x_{CHO}) was fixed at 0.00, 0.35, 0.40, and 0.50). So, the parallel existence of superlattices at the lipid headgroup and at the acyl chain levels is feasible [68]. Headgroup superlattice (SL) model, suggests that phospholipid headgroups of different structures tend to adopt regular distributions even in the presence of CHO [68].

Interestingly, SL were associated to deviations in drug partitioning [69] and fluorescence anisotropy [70]. Not only these phenomena but also the increased tendency to lipid channel formation and temporally auto-correlated membrane behavior described in the present work can lead to consider that, similarly to what happens in phase coexistence conditions, the SL organization provide the bilayers with discontinuities (defects) in the molecular packing which, upon perturbation, favors lipid channel like behavior through the increase in the number and/or size of water domains.

4.5. The complex mixture of lipids from synaptosomal membrane exhibits a smooth current fluctuation

These results reflected the higher stability of BLM_{bSM} compared with BLM_0. Interestingly, the sensitivity of BLM_{SM} to the transmembrane potential was significantly lower than that of binary phospholipid mixture POPE:POPC (7:3) suggesting that compensation of molecular geometries in the complex SM lipid mixture may be responsible for dumping ionic currents. This hypothesis will be further investigated in future studies.

5. Conclusions

The present study was based on the hypothesis that some aspects of the membrane structural dynamics are encoded within the pattern of temporal fluctuations in ion currents. So, using the BLM model, membranes of varied compositions were perturbed by applying a ΔV. It was assumed that nonzero conductance is due to the opening of lipid channels. The perturbation threshold decreased with the CHO content of the membrane. This was evidenced by the increase in the magnitude of I, the number of conductance states and the variability in the shape of the fluctuation patterns. The latter leaded to a systematic study applying a global characterization method that allowed describing the autocorrelation structure of the time series which was synthesized in the self-similarity parameter α. A similar rationale was applied to the analysis of timescales of channels open times. These analyses were rationalized as pores behaving independently at low voltages in CHO free membranes and becoming temporally autocorrelated as ΔV and CHO content increased. It was concluded that pores grew up either in size and/or in number up to the point at which they started working as an interconnected network. This effect expanded (percolated) to the whole membrane and, at extreme conditions of ΔV, led to the breaking up of the membrane. This suggests that lipid pores behave as a spatio-temporal correlated phenomenon. Percolation could be achieved at lower voltages, thus requiring less energy, in membranes containing CHO. Voltage induced changes in membrane capacitance (C_m) revealed the increase in the polarity of the membrane core (ε increased) in the presence of CHO.

It is worth noting that in the present study, channel-like behavior was observed in fluid membranes which means in the absence of phase coexistence. However, the phospholipid/CHO mixtures were used at compositions known to be structurally organized in what are known as superlattices which are derived from frustration of packing. Consequently, a generalization allowed by the present results is that the onset of channel-like behavior in lipid membranes requires the presence of packing defects. BLM_{bSM} composed of the complex mixture of Folch's lipid extract were almost insensitive within the same ΔV range used to perturb the other BLMs. This would imply the absence of defects in the packing structure and/or the compensation of geometries among the multiple molecular identities comprising this complex mixture.

Pure lipid membranes are matrices where channel- or pore-forming proteins are usually inserted. It should be realized that the matrix behavior is expected to be perturbed as a whole in the presence of proteins. So the current fluctuation behavior of protein free membrane cannot, in principle, be taken as a background signal to be discounted from the protein containing membrane. Each system should be considered as an individual entity. So, the question that arises is how to apply lessons learned from simple model membranes to actual biomembranes.

Biological membranes are complex mixtures of lipids with different melting points and different hydrophobic lengths, including CHO and

proteins, and exhibit phase separation and domain formation phenomena. Therefore, one must expect that fluctuations display different magnitude in different membrane regions with intensities that depend on the length scale over which they are monitored, the whole membrane or in windows of smaller size, e.g. on the length scale of individual domains or on molecular scale. So, biomembrane would exhibit a complex mixture of fluctuation frequencies and patterns, most of which would come from packing defects.

Acknowledgements

Authors gratefully acknowledge Prof. B. Maggio and Dr. M.A. Aon for their helpful discussions, Drs. H. Cantiello and R. Cantero for helping us with the experimental setup at the early stages of our work and Ivan Felsztyna for his technical assistance. Present study was supported by grants from CONICET, SeCyT-UNC, Mincyt-Provincia de Córdoba and ANPCyT. NAC and PDC are graduate students of the Doctorado en Ciencias Biológicas, FCEFyN, UNC. PDC and NAC hold fellowships from CONICET (Argentina). JMK and MAP are career members of the later institution.

Appendix A. Supplementary data

Supplementary data to this article can be found online at http://dx.doi.org/10.1016/j.bbamem.2013.03.019.

References

[1] E.A. Disalvo, F. Lairion, F. Martini, E. Tymczyszyn, M. Frias, H. Almaleck, G.J. Gordillo, Structural and functional properties of hydration and confined water in membrane interfaces, Biochim. Biophys. Acta 1778 (2008) 2655–2670.
[2] T. Heimburg, Review: lipid, ion channels, arXiv:1001.2524v114 Jan 2010, (physics.bio-ph).
[3] M.M. Cox, D.L. Nelson, Lehninger. Principios de bioquímica, 5 ed. Omega, 2009.
[4] M.d.R. Cantero, H.F. Cantiello, Effect of lithium on the electrical properties of polycystin-2 (TRPP2), Eur. Biophys. J. 40 (2011) 1029–1042.
[5] R. Latorre, O. Alvarez, Voltage-dependent channels in planar lipid bilayer membranes, Physiol. Rev. 61 (1981) 77–150.
[6] O.P. Hamill, B. Martinac, Molecular basis of mechanotransduction in living cells, Physiol. Rev. 81 (2001) 685–740.
[7] H.J. Seeger, L. Aldrovandi, A. Alessandrini, P. Facci, Changes in single K^+ channel behavior induced by a lipid phase transition, Biophys. J. 99 (2010) 3675–3683.
[8] D. Papahadjopoulos, K. Jacobson, S. Nir, T. Isac, Phase transitions in phospholipid vesicles, fluorescence polarization and permeability measurements concerning the effect of temperature and cholesterol, Biochim. Biophys. Acta 311 (1973) 330–340.
[9] B. Maggio, M.G. Mestrallet, F.A. Cumar, R. Caputto, Glucose release from liposomes containing gangliosides or other membrane lipids induced by biogenic amines and myelin basic protein, Biochem. Biophys. Res. Commun. 77 (1977) 1265–1272.
[10] V.F. Antonov, A.A. Anosov, V.P. Norik, E. Smirnova, A soft poration of planar bilayer lipid membranes from dipalmitoylphosphatidylcholine at the temperature of the phase transition from the liquid crystalline to the gel state, Biofizika 50 (2005) 867–877.
[11] V.F. Antonov, V.V. Petrov, A.A. Molnar, D.A. Predvoditelev, A.S. Ivanov, The appearance of single ion channels in unmodified lipid bilayer membrane at the phase transition temperature, Nature 283 (1980) 585–588.
[12] A. Blicher, K. Wodzinska, K. Fidorra, M. Winterhalter, T. Heimburg, The temperature dependence of lipid membrane permeability, its quantized nature, and the influence of anesthetics, Biophys. J. 96 (2009) 4581–4591.
[13] J. Gallaher, K. Wodzińska, T. Heimburg, M. Bier, Ion-channel-like behavior in lipid bilayer membranes at the melting transition, Phys. Rev. E 81 (2010), (061925–061921 - 061625–061925).
[14] K. Wodzinska, A. Blicher, T. Heimburg, The thermodynamics of lipid ion channel formation in the absence and presence of anesthetics. BLM experiments and simulations, Soft Matter 5 (2009) 3319–3330.
[15] B. Wunderlich, C. Leirer, A.-L. Idzko, U.F. Keyser, A. Wixforth, V.M. Myles, T. Heimburg, M.F. Schneider, Phase-state dependent current fluctuations in pure lipid membranes, Biophys. J. 96 (2009) 4592–4597.
[16] L. Delemotte, M. Tarek, Molecular dynamics simulations of lipid membrane electroporation, J. Membr. Biol. (2012), http://dx.doi.org/10.1007/s00232-012-9434-6.
[17] K.C. Melikov, V.A. Frolov, A. Shcherbakov, A.V. Samsonov, Y.A. Chizmadzhev, L.V. Chernomordik, Voltage-induced nonconductive pre-pores and metastable single pores in unmodified planar lipid bilayer, Biophys. J. 80 (2001) 1829–1836.
[18] S. Samanta, J. Stiban, T.K. Maugel, M. Colombini, Visualization of ceramide channels by transmission electron microscopy, BBA-Bioenerg. 1808 (2011) 1196–1201.
[19] C. Shao, B. Sun, D.L. DeVoe, M. Colombini, Dynamics of ceramide channels detected using a microfluidic system, PLoS One 7 (2012) e43513.
[20] A. Carruthers, D.L. Melchior, Transport of alpha- and beta-D-glucose by the intact human red cell, Biochemistry 24 (1985) 4244–4250.
[21] S.A. Freeman, M.A. Wang, J.C. Weavert, Theory of electroporation of planar bilayer membranes: predictions of the aqueous area, change in capacitance, and pore–pore separation, Biophys. J. 67 (1994) 42–56.
[22] C.D. Stubbs, S.J. Slater, The effects of non-lamellar forming lipids on membrane protein–lipid interactions, Chem. Phys. Lipids 81 (1996) 185–195.
[23] M. Bogdanov, W. Dowhan, Phosphatidylethanolamine is required for in vivo function of the membrane-associated lactose permease of *Escherichia coli*, Biol. Chem. 270 (1995) 732–739.
[24] E. van den Brink-van del Laan, J.A. Killian, B. De Kruijff, Nonbilayer lipids affect peripheral and integral membrane proteins via changes in the lateral pressure profile, Biochim. Biophys. Acta 1666 (2004) 275–288.
[25] R.S. Cantor, Lateral pressures in cell membranes: a mechanism for modulation of protein function, J. Phys. Chem. B 101 (1997) 1723–1725.
[26] C.H., Mdel R. Cantero, Effect of lithium on the electrical properties of polycystin-2 (TRPP2), Eur. Biophys. J. 40 (2011) 1029–1042.
[27] S.G. González-Perrett, K. Kim, C. Ibarra, A.E. Damiano, E. Zotta, M. Batelli, P.C. Harris, I.L. Reisin, M.A. Arnaout, H.F. Cantiello, Polycystin-2, the protein mutated in autosomal dominant polycystic kidney disease (ADPKD), is a Ca^{2+}-permeable nonselective cation channel, Proc. Natl. Acad. Sci. U.S.A. 98 (2001) 1182–1187.
[28] D. Schmidt, Q.X. Jiang, R. MacKinnon, Phospholipids and the origin of cationic gating charges in voltage sensors, Nature 444 (2006) 775–779.
[29] D.A. Pink, S. McNeil, B. Quinn, M.J. Zuckermann, A model of hydrogen bond formation in phosphatidylethanolamine bilayers, Biochim. Biophys. Acta 1368 (1998) 289–305.
[30] W. Pohle, C. Selle, H. Fritzsche, M. Bohl, Comparative FTIR spectroscopic study upon the hydration of lecithins and cephalins, J. Mol. Struct. 408/409 (1997) 273–277.
[31] B. Hoop, C.K. Peng, Fluctuations and fractal noise in biological membranes, J. Membr. Biol. 177 (2000) 177–185.
[32] L.S. Liebovitch, D. Scheurle, M. Rusek, M. Zochowski, Fractal methods to analyze ion channel kinetics, Methods 24 (2001) 359–375.
[33] D.M. Dominguez, M. Marin, M. Camacho, Macrophage ion currents are fit by a fractional model and therefore are a time series with memory, Eur Biophys J. 38 (2009) 457–464.
[34] S.M. Bezrukov, M. Winterhalter, Examining noise sources at the single-molecule level: 1/f noise of an open maltoporin channel, Phys. Rev. Lett. 85 (2000) 202–205.
[35] A.R. Brazhe, G.V. Maksimov, Self-organized critical gating of ion channels: on the origin of long-term memory in dwell time series, Chaos 16 (2006) 033129.
[36] J.K. Chui, T.M. Fyles, Apparent fractal distribution of open durations in cyclodextrin-based ion channels, Chem. Commun. (Camb.) 46 (2010) 4169–4171.
[37] S. Mercik, K. Weron, Stochastic origins of the long-range correlations of ionic current fluctuations in membrane channels, Phys. Rev. E Stat. Nonlinear Soft Matter Phys. 63 (2001) 051910.
[38] Z. Siwy, A. Fulinski, Origin of 1/f(alpha) noise in membrane channel currents, Phys. Rev. Lett. 89 (2002) 158101.
[39] F. Wohnsland, R. Benz, 1/f-Noise of open bacterial porin channels, J. Membr. Biol. 158 (1997) 77–85.
[40] M. Bier, J. Gallaher, Ion traffic through a cell membrane - and how its 1/f noise connects to Gambler's ruin, Catalan numbers and Zipf's law, Fluct. Noise Lett. 10 (2011) 419–430.
[41] J. Folch, M. Lees, G.H. Sloane-Stanley, A simple method for the isolation and purification of total lipids from animal tissues, J. Biol. Chem. 226 (1957) 497–509.
[42] A.V. Turina, S. Schreier, M.A. Perillo, Coupling between GABAA-R ligand-binding activity and membrane organization in β-cyclodextrin-treated synaptosomal membranes from bovine brain cortex: new insights from EPR experiments, Cell. Biochem. Biophys. 63 (2012) 17–33.
[43] M.A. Perillo, A. Arce, Determination of the membrane-buffer partition coefficient of flunitrazepam, a lipophilic drug, J. Neurosci. Methods 36 (1991) 203–208.
[44] D. Marsh, Lateral pressure in membranes, Biochim. Biophys. Acta 1283 (1996) 183–223.
[45] O. Alvarez, E. Diaz, R. Latorre, Voltage-dependent conductance induced by hemocyanin in black lipid films, Biochim. Biophys. Acta 389 (1975) 444–448.
[46] A.J. Williams, An introduction to the methods available for ion channel reconstitution, in: D. Ogden (Ed.), Microelectrode Techniques, The Plymouth Workshop Handbook, The Company of Biologists Limited, Cambridge, 1994, pp. 79–99.
[47] J.M. Kembro, M.A. Perillo, R.H. Marin, Análisis de fluctuación con eliminación de tendencias en estudios de comportamiento animal: los efectos de la inactividad inducida por estrés, Actas Acad. Nac. Cienc. Cordoba XIV (2008) 108–116.
[48] J.M. Kembro, D.G. Satterlee, J.B. Schmidt, M.A. Perillo, R.H. Marin, Open-field temporal pattern of ambulation in Japanese quail genetically selected for contrasting adrenocortical responsiveness to brief manual restraint, Poult. Sci. 87 (2008) 2186–2195.
[49] C.K. Peng, S.V. Buldyrev, S. Havlin, M. Simons, H.E. Stanley, A.L. Goldberger, Mosaic organization of DNA nucleotides, Phys. Rev. E Stat. Nonlinear Soft Matter Phys. 49 (1994) 1685–1689.
[50] C.K. Peng, J.M. Hausdorff, A.L. Goldberger, Fractal mechanisms in neural control: human heartbeat and gait dynamics in health and disease, in: J. Walleczek (Ed.), Self-Organized Biological Dynamics and Nonlinear Control, Cambridge University Press, 2000, pp. 66–96.
[51] K.M. Rutherford, M.J. Haskell, C. Glasbey, A.B. Lawrence, The responses of growing pigs to a chronic–intermittent stress treatment, Physiol. Behav. 89 (2006) 670–680.
[52] J.W. Kantelhard, E. Koscielny-Bunde, H.H.A. Rego, S. Havlin, A. Bunde, Detecting long-range correlations with detrended fluctuation analysis, Phys. A 295 (2001) 441–454.
[53] E. Milotti, 1/f noise: a pedagogical review, arXiv:physics/02040332002.
[54] R.R. Sokal, F.J. Rohlf, Biometry: The Principles and Practice of Statistics in Biological Research, 4th ed. Freeman, W.H. and Co., New York, 2012.
[55] J.A. Di Rienzo, F. Casanoves, M.G. Balzarini, L. Gonzalez, M. Tablada, C.W. Robledo, InfoStat, 2011.

[56] O. Alvarez, R. Latorre, Voltage-dependent capacitance in lipid bilayers made from monolayers, Biophys. J. 21 (1978) 1–17.
[57] S.H. White, W. Chang, Voltage dependence of the capacitance and area of black lipid membranes, Biophys. J. 36 (1981) 449–453.
[58] J.M. Hausdorff, C. Peng, Multiscaled randomness: a possible source of 1/f noise in biology, Phys. Rev. E Stat. Phys. Plasmas Fluids Relat. Interdiscip. Topics 54 (1996) 2154–2157.
[59] V.F. Antonov, A.A. Anosov, V.P. Norik, E.A. Korepanova, E.Y. Smirnova, Electrical capacitance of lipid bilayer membranes of hydrogenated egg lecithin at the temperature phase transition, Eur. Biophys. J. 32 (2003) 55–59.
[60] T. Heimburg, The capacitance and electromechanical coupling of lipid membranes close to transitions: the effect of electrostriction, Biophys. J. 103 (2012) 918–929.
[61] H. Almaleck, G.J. Gordillo, A. Disalvo, Water defects induced by expansion and electrical fields in DMPC and DMPE monolayers: contribution of hydration and confined water, Colloids Surf. B Biointerfaces 102 (2013) 871–878.
[62] K. Kaufmann, W. Hanke, A. Corcia, Ion channel fluctuations in pure lipid bilayer membranes: control by voltage, K.Kaufmann, Caruaru, Brazil, 1989.
[63] D. Papahadjopoulos, J.C. Watkins, Phospholipid model membranes. II. Permeability properties of hydrated liquid crystals, Biochim. Biophys. Acta 135 (1967) 639–652.
[64] R. Kraayenhof, G.J. Sterk, W. Harro, F.S. Wong, K. Krab, R.M. Epand, Monovalent cations differentially affect membrane surface properties and membrane curvature, as revealed by fluorescent probes and dynamic light scattering, Biochim. Biophys. Acta 1282 (1996) 293–302.
[65] H. Leontiadou, A.E. Mark, S.-J. Marrink, Ion transport across transmembrane pores, Biophys. J. 92 (2007) 4209–4215.
[66] K.H. Cheng, M. Ruonala, J. Virtanen, P. Somerharju, Evidence for superlattice arrangements in fluid phosphatidylcholine/phosphatidylethanolamine bilayers, Biophys. J. 73 (1997) 1967–1976.
[67] B. Cannon, G. Heath, J. Huang, P. Somerharju, J.A. Virtanen, K.H. Cheng, Time-resolved fluorescence and Fourier transform infrared spectroscopic investigations of lateral packing defects and superlattice domains in compositionally uniform cholesterol/phosphatidylcholine bilayers, Biophys. J. 84 (2003) 3777–3791.
[68] B. Cannon, A. Lewis, J. Metze, V. Thiagarajan, M.W. Vaughn, P. Somerharju, J. Virtanen, J. Huang, K.H. Cheng, Cholesterol supports headgroup superlattice domain formation in fluid phospholipid/cholesterol bilayers, J. Phys. Chem. B 110 (2006) 6339–6350.
[69] M.M. Wang, I.P. Sugar, P.L. Chong, Role of the sterol superlattice in the partitioning of the antifungal drug nystatin into lipid membranes, Biochemistry 37 (1998) 11797–11805.
[70] K.H. Cheng, J. Virtanen, P. Somerharju, Fluorescence studies of dehydroergosterol in phosphatidylethanolamine/phosphatidylcholine bilayers, Biophys. J. 77 (1999) 3108–3119.